

# Urban 5G MmWave Networks: Line-of-Sight Probabilities and Optimal Site Locations

---

**Tian Han**

Department of Electrical and Electronic Engineering, University of Melbourne

**Davood Shojaei**

Centre for SDIs and Land Administration, Department of Infrastructure Engineering, University of Melbourne

**Paul Fitzpatrick**

Telstra Corporation  
Department of Electrical and Electronic Engineering, University of Melbourne

**Taka Sakurai**

Telstra Corporation  
Department of Electrical and Electronic Engineering, University of Melbourne

**Jamie Evans**

Department of Electrical and Electronic Engineering, University of Melbourne

---

**Abstract:** In this work, we implemented line-of-sight (LoS) ray tracing functionality to investigate problems in millimetre-wave propagation modelling and network planning in 3D city model environments. First, we validated an existing LoS propagation probability model expressed as an exponential rule with the link distance. By fitting ray tracing simulation results under different scenarios to the model, the relationships between key parameters in the model and factors including the building density and the transmitter height were qualitatively analysed. Next, we developed a network planning framework for a multi-hop outdoor urban network by formulating a mixed-integer linear programming problem which minimises the overall deployment cost through optimal site selection. Taking the sets of potential site locations and potential links as inputs, we selected a subset of the sites that comprise a tree-structured network that satisfies all the user demands at a minimum deployment cost. We also analysed the time required for solving this optimisation problem in order to provide a prediction of the execution time for larger-sized problems.

**Keywords:** Ray tracing, line-of-sight communications, network planning, mixed-integer linear programming, 3D visualisation.

## Introduction

The fifth generation (5G) wireless networks are expected to deliver high data rates with low latency and high spectral efficiency to support the rapid increase in mobile data demand ([Anjinappa et al., 2021](#); [Rappaport et al., 2013](#)). In order to overcome spectrum scarcity and provide wider bandwidths ranging from hundreds of megahertz (MHz) to several gigahertz (GHz) ([He et al., 2019](#); [Rappaport et al., 2013](#); [Rangan et al., 2014](#)), 5G needs to expand into the under-utilised millimetre-wave (mmWave) bands between 30 GHz to 300 GHz, or more generally, above 10 GHz. However, compared to the traditionally used sub-6 GHz frequency bands, mmWave bands present new challenges for network design.

The path loss is greater for the mmWave bands and propagation is also susceptible to blockage from buildings and foliage, making performance highly location-specific. Due to this high path loss and the paucity of useful reflected paths, line-of-sight (LoS) propagation assumes far greater importance than non-line-of-site (NLoS) propagation at mmWave ([Al-Hourani, 2020](#); [Cui et al., 2020](#)). The significant difference in path loss between LoS and NLoS paths is also evident from existing stochastic propagation models ([Baum et al., 2005](#); [Meinila et al., 2009](#)). Stochastic propagation models use a LoS probability parameter to account for variation in the occurrence of LoS in different environments; this parameter has a significant influence on the distribution of received signal strength and is therefore important to validate. One way to validate the LoS probability is to use ray tracing, which is the approach taken in this work. Ray tracing (RT) is considered an indispensable tool for modelling mmWave propagation in specific environments due to its accuracy ([He et al., 2019](#)).

The challenges of mmWave propagation drive network densification, meaning a significant increase in the number of cell sites to provide mmWave coverage. Network densification complicates the design because it may be cost prohibitive to provide high-capacity fibre connections, i.e., fibre points of presence (fibre PoP), at the potentially large number of mmWave cell sites. This, in turn, leads to a need for alternate back-haul architectures that provide the interconnection between the fibre PoPs and the cell sites to enable a cost effective network deployment. For example, relay nodes that extend the high-speed connection from the fibre PoPs to the mmWave cell sites are considered. These nodes use frequencies in the mmWave band to provide a high-capacity link between the fibre PoP and the cell site. Cost effective mmWave network design relies on identifying the set of node locations from the set of candidate locations that leads to the lowest cost network.

## Problem Description

This work considers a mmWave network comprised of four node types. The set of potential fibre PoPs that can provide the high-speed connection to the mmWave network is  $\mathcal{FP}$ . The set of potential sites for relay nodes is  $\mathcal{PS}$ . These nodes provide the connection from the fibre PoPs to either (i) other relay nodes or (ii) to a cell site. The set of demand nodes that represent the traffic demand from users connected to mmWave cell sites is  $\mathcal{DN}$ . Demand nodes require a connection directly to a fibre PoP or via relay nodes. Finally, there is a singleton set,  $\mathcal{SS}$ , containing a virtual super source node, which can be viewed as the gateway between the designed network and the outer network. Thus, this node is the root of the resulting tree comprising the other three node types.

The goal is to identify the optimal locations for nodes given the sets  $\mathcal{FP}$ ,  $\mathcal{PS}$ ,  $\mathcal{DN}$  and  $\mathcal{SS}$ . This should be solved quickly because of the potential number of nodes and sites needed for a large network. Figure 1 gives an example of the structure of the resulting network. Since the links between these nodes use the mmWave band, signal propagation plays a key role in identifying node locations, as the distance between nodes should be maximised to reduce the number of nodes whilst still providing low loss to achieve high data rate transmission between the nodes.

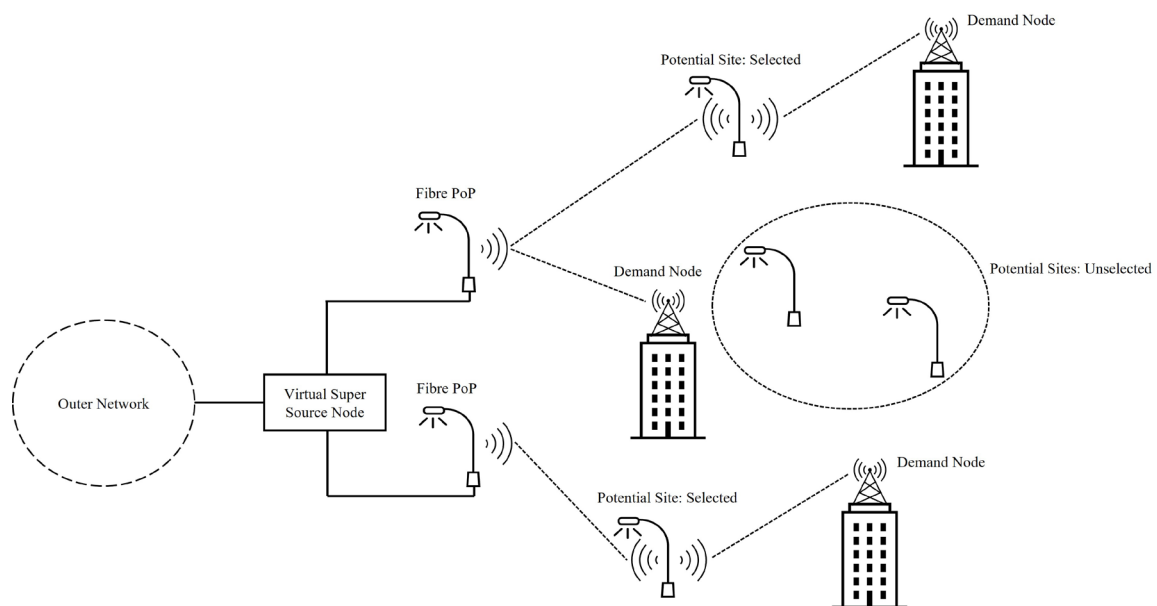


**Figure 1.** An example of the resulting network.

Among different propagation modelling methods, RT has been considered as a suitable candidate (Al-Hourani, 2020; Cui et al., 2020). It performs simulation based on three-dimensional (3D) environment data in order to track propagation paths. To be more specific, RT can be employed to assist in the propagation modelling by identifying LoS and NLoS paths. Selecting nodes where the propagation between them is LoS removes those with NLoS paths

where signal losses are higher and potentially intermittent due to blockages and so favours higher quality connections with greater capacity and reliability.

## Scope and Contribution

The contribution of this work includes the validation of an existing LoS probability model and the development of an urban area site selection tool based on 3D city models. More specifically, we develop a ray tracer in Cesium ([Cesium, 2015a](#)) in which only LoS paths are considered, since NLoS paths are less reliable and inferior compared to LoS paths. Although specular reflections are also considered in many ray tracers for higher accuracy ([He et al., 2019](#); [Zhang et al., 2015](#); [Lai et al., 2019](#); [Lecci et al., 2021](#), [Lecci et al., 2020](#); [Bodi et al., 2021](#)), due to the high penetration loss and the lack of useful reflected paths in mmWave frequency bands, considering only LoS communication provides a useful lower bound on performance.

Using the LoS checking functionality, we developed a LoS probability simulation tool and performed simulations in several Australian downtown areas based on 3D environment data in order to evaluate a theoretical urban area LoS probability model ([Andrews et al., 2017](#)) and to investigate factors that impact the model parameters.

Next, we developed a network planning tool by formulating a mixed-integer linear programming problem to minimise the overall deployment cost by proper site selection in part of the Melbourne central business district (CBD). The implemented ray tracer checks possible LoS transmissions and provides the length of each link. From these lengths, key metrics such as signal-to-noise ratio (SNR) and link capacity are calculated. Considering the link capacity and the network structure as constraints, the site selection optimisation problem is solved using an existing solver in Matlab and the result is visualised in Cesium.

## Methodology

The development of the ray tracer and the RT based planning tool prototype has three stages:

- Review of the existing works that are relevant to RT-based LoS probability validation and network planning ([Related Works](#)).
- Design and development of the ray tracer as well as a prototype with the functionalities of LoS probability validation and network planning ([Design and Development](#)).
- Evaluation of the developed prototype planning tool based on the analysis of the results of various case studies ([Case Study](#)).

## Related Works

### Ray Tracing for LoS Probability Model Validation

The existing literature proposes several RT-based methods for LoS probability calculation. In Al-Hourani ([2020](#)), a model for predicting the geometric LoS in different urban environments is formulated based on stochastic geometry in which the existence of buildings is modelled as points following the Poisson point process (PPP). The model is then verified using RT-based Monte-Carlo simulations, which show a high degree of agreement between the simulation results and the theoretical analysis. In Cui *et al.* ([2020](#)), a frequency-dependent LoS probability model is proposed. RT-based numerical simulations are presented to show the accuracy of the proposed model.

Apart from the buildings, the blockage caused by vegetation or the human body is also of interest. In Thomas *et al.* ([2014](#)), RT is used to come up with a distance-based blocking probability function representing blockage by other users and foliage in an outdoor mmWave local area access system. By fitting from simulation results, it was found that the blockage probability is a linear function of the link length. In Thomas *et al.* ([2016](#)), the LoS probability model under the LoS-foliage case is verified using RT technology, in which the blockage caused by foliage but not buildings is considered as a third state apart from LoS and NLoS. It is found that the NYU-squared LoS probability model ([Aalto et al., 2016](#)) gives a low mean squared error when compared to the RT results.

### Ray Tracing for Network Planning

RT-based mmWave network design is a two-stage problem ([Danford et al., 2017](#)). Firstly, RT needs to be executed in a given geospatial dataset in order to characterise the communication environment. Based on the results computed by RT, the second step is to use mathematical models to formulate the design as an optimisation problem and utilise tools from optimisation theory to find a solution ([Kennington et al., 2011](#)). From the perspective of the first step, a large body of research has been conducted on characterising the communication environment using RT. In 1991, researchers have considered RT as a design tool in radio networks ([McKown& Hamilton, 1991](#)). Efficient algorithms were developed to approximate wave propagation and calculate two-dimensional (2D) coverage maps that provide visualisation to the received power at different locations. Similarly, a ray tracer was implemented to calculate the coverage map in an indoor environment in ([Ashour et al., 2016](#)). An enhanced RT algorithm was proposed that evaluates the relative change in coverage associated with displacement of the antenna location of a previously computed solution, which improves the computational complexity without sacrificing the accuracy. In Mellios *et al.* ([2012](#)), a 3D ray-

tracing tool is combined with real-world measurements in order to derive a set of urban macrocell propagation statistics suitable for Long Term Evolution (LTE) cellular network planning. The RT study is performed in two different urban environments and the results are compared with the WINNER II/+ standardised channel model ([Jamsa et al., 2016](#)).

Generally speaking, the network design problem is complex and composed of multiple aspects. One subproblem is the site selection optimisation problem, which aims to find a subgraph of a graph formed by a set of given nodes and links in order to optimise an objective function while satisfying certain constraints ([Danford et al., 2017](#)). This is a classical problem that is studied in a wide range of applications, for example, communications network planning. In [Kennington et al. \(2011\)](#), the state-of-the-art optimisation methods for design, analysis and management of wireless networks including cellular and wireless local area networks (LANs) are surveyed. In [Benyamina et al. \(2012\)](#), different aspects of wireless mesh network design are discussed. Methods which are proposed to improve the performance of an existing network or to improve its performance by a careful planning of its deployment are examined. Motivated by the development of Facebook's backhaul technology named Terragraph ([Choubey & Yazdan, 2016](#)), a suite of tools to support the design and end-to-end planning of fixed 60 GHz mmWave backhaul and access networks is proposed in [Danford et al. \(2017\)](#). Given light detection and ranging (LiDAR) data representing the environment, the site locations are generated using 3D computer vision and the potential links are determined based on a LiDAR-specific LoS analysis algorithm. The graph formed by the resulting sites and links is then sent into an optimisation algorithm developed based on the Steiner tree problem ([Winter, 1987](#)), in order to minimise the deployment cost and satisfy the user demands by finding a subgraph. Very few works in the literature have incorporated a real 3D city to study the impact of the surrounding environment on the parameters of LoS probability models. Furthermore, as far as we are aware, the aforementioned [Danford et al. \(2017\)](#) is the only study that has combined 3D model-based RT technology with the site selection optimisation problem for network planning. Thus, this area requires more exploration to understand the potential and challenges of using 3D models for these analyses. In this paper, we aim to develop an RT prototype in order to analyse a theoretical LoS probability model and perform optimisation of site selection in real 3D city models.

## Design and Development of the Prototype

In this work, we developed a prototype that has two functionalities. Firstly, it can calculate the LoS probability with distance in an area of interest based on extensive RT simulations. The simulation results are then used to evaluate an existing LoS probability model ([Andrews et al., 2017](#)) and investigate factors that impact the model parameters. Secondly, a network planning

tool is implemented in this prototype, which minimises the overall cost of network deployment by selecting a proper subset of given candidate site locations. This is achieved by formulating a mixed-integer linear programming problem. Both functionalities are based on an implemented simple ray tracer. Before describing the development of the prototype, we review some important issues including the platform and datasets.

## Platform

The prototype is mainly implemented in Cesium, which is an open-source platform for creating powerful 3D geospatial applications ([Cesium, 2015a](#)). It allows users to combine their own 3D data with the provided global content. The open-source JavaScript library, CesiumJS, allows users to create interactive web applications for dynamic geospatial data sharing and accurate 3D visualisation-based analysis.

While Cesium provides good visualisation of a 3D environment, it is not suitable for intensive mathematical calculations. In this work, we consider Matlab for this purpose.

For the LoS probability model validation functionality, the model is fitted to simulation results using Matlab. For the network planning functionality, the optimisation is performed using Matlab Optimisation Toolbox, which provides functions for finding parameters that minimise or maximise objective functions while satisfying constraints ([MathWorks, 2022](#)).

In order to link the two platforms, the data transfer between them is critical. In this prototype, the data is transferred by .csv files, since both platforms support this file format.

## Data

To model the 3D environment dataset, we used OSM Buildings ([Cesium, 2015b](#)), which is a 3D buildings layer covering the entire world. It is available as a 3D Tileset and ready to be used in custom applications with CesiumJS or any client that supports 3D Tiles. It is derived from OpenStreetMap and contains over 350 million buildings with per-building metadata. This includes basic information like building name and height, address, opening hours, and even type of material for individual parts of buildings.

Apart from the 3D environment, the data of potential locations where the sites can be deployed is also necessary in the network planning problem. In a fixed backhaul and access network, the sites are usually set up on street furniture such as streetlights. However, the street furniture is not included in the Cesium OSM Building dataset; thus the potential locations are not available. Therefore, in this prototype the potential site locations are synthesised according to some rules which are described in the [case study](#).

## Utility

This prototype can be used for various purposes. Researchers focusing on the study of LoS probability models can evaluate their theoretical analysis using the LoS probability functionality, while mobile network operators can estimate the network performance in a given environment. Network operators can also use the network planning functionality for site selection.

## Design and Development

### Ray Tracer

The ray tracer is able to check the existence of LoS between the given locations of a transmitter (Tx) and a receiver (Rx). The flow chart in Figure 2 shows how to check the existence of LoS between a Tx and an Rx. A CesiumJS function named "*viewer.scene.pickFromRay()*" is used to generate a ray based on the location of the Tx and the direction from the Tx to the Rx. It returns the intersection of the ray and the 3D environment. The existence of LoS is checked by comparing the distance between the Tx and the Rx with that between the Tx and the intersection.

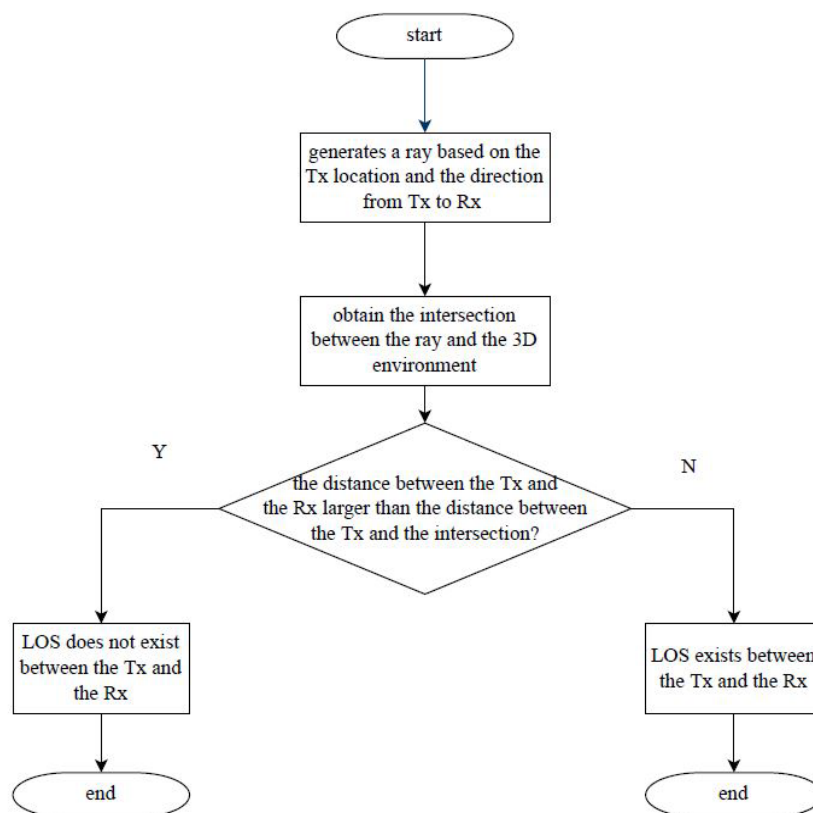


**Figure 2.** Flow chart of checking the existence of LoS between a Tx and an Rx.



## LoS Probability Validation

The problem of modelling LoS probability or blockage probability is of great interest due to the importance of LoS communication in mmWave transmission ([Al-Hourani, 2020](#)). A function  $P_{\text{LoS}}(d)$  is a deterministic non-increasing function that takes values in  $[0,1]$  and is interpreted as the probability that an arbitrary link of length  $d$  is LoS. A typical model for the probability in urban areas is given as ([Andrews et al 2017](#)):

$$P_{\text{LoS}}(d) = \min\left(\frac{A}{d}, 1\right) (1 - e^{-d/E}) + e^{-d/E}, \quad (1)$$

where  $A$  is a threshold distance and  $E$  affects the speed of decay with distance  $d$ . Though the exact values of  $A$  and  $E$  vary depending on the exact environment, we should notice that the model in (1) always follows an exponential rule with distance. Theoretical works, such as Al-Hourani ([2020](#)) and Bai *et al.* ([2014](#)), study the reason behind the exponential models under different scenarios where the existence of the buildings follows the PPP.

In order to evaluate the exponential model and study the possible factors that affect the parameters in (1), we perform simulations in Cesium to calculate the LoS probability in different circumstances. For a particular distance  $d$ , the Tx and Rx locations are guaranteed to be  $d$  apart, but randomly chosen for a certain number of iterations. For each Tx-Rx pair, the implemented ray tracer checks the existence of LoS using the implemented ray tracer following the procedure in Figure 2. The LoS probability at distance  $d$  is determined by the fraction of iterations where LoS exists. Next, we fit the simulation outcomes to the model in (1) using Matlab in order to calculate the parameters  $A$  and  $E$ .

## Deployment Cost Optimisation in Network Planning

In this section, we follow the work in Danford *et al.* ([2017](#)) and propose a fixed wireless network planning tool which minimises the total deployment cost while satisfying a variety of constraints, including user demands, link capacity and the structure and balance of the network. A flow chart is provided in Figure 3 to describe the main process of this tool.

Suppose the locations of fibre points-of-presence (PoPs), potential sites and demand nodes are given. A fibre PoP is a node equipped with fibre, which can be viewed as the gateway between the outer core network and the local access network that we are interested in. A potential site is a possible location to deploy a relay node, which decodes the received signal and then re-transmits the message to other nodes. A demand node is placed at the rooftop of a particular building and represents the demand from multiple users in this building. These nodes form a network that enables transmission between fibre PoPs and demand nodes in order to satisfy all the demands. In this prototype, we only consider downlink communications, in which the network traffic comes from the outer core network, goes

through the fibre PoPs and finally arrives at the demand nodes. We assume that a transmission can only be achieved via LoS links with distance below a predefined threshold,  $d_{\max}$ . Furthermore, communications are only allowed between a fibre PoP and a relay node, a fibre PoP and a demand node, two relay nodes or a relay node and a demand node. The LoS links are checked using the ray tracer in Cesium based on the method in Figure 2.

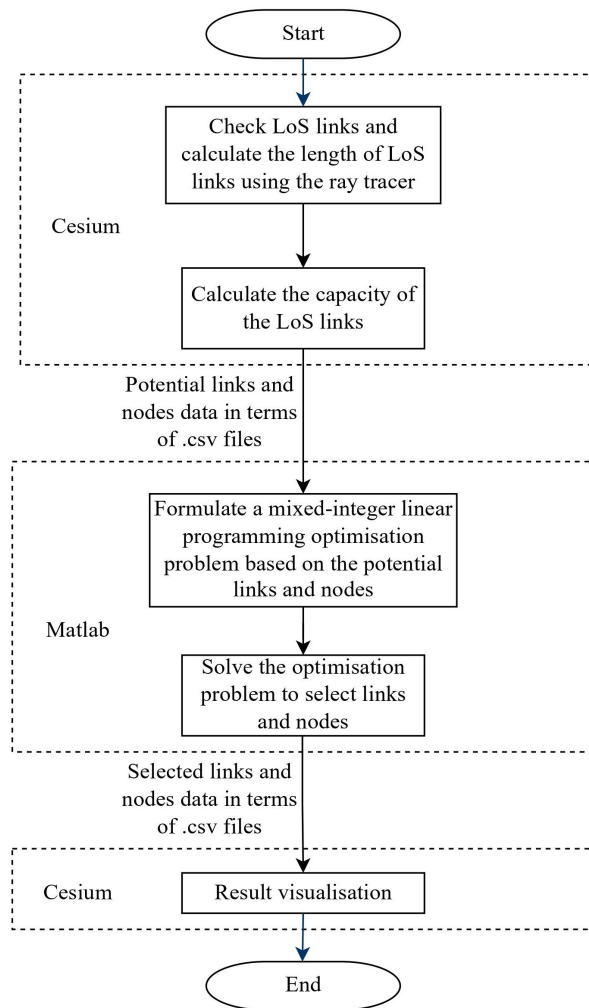


**Figure 3.** Flow chart of the network planning tool.

The problem of searching for a site selection that minimises the deployment cost can be formulated as an optimisation problem. Before formulating the optimisation problem, we need to specify some key metrics in the network.

- a) Cost: the costs of deploying a fibre node or a relay node are different. Since this prototype focuses more on site selection rather than the total deployment cost, we assume that the cost of deploying a fibre PoP is approximately twice the cost of deploying a relay node (Lalwani, 2018) without using the exact deployment cost.
- b) Capacity: we assume that the capacity of a link between node  $i$  and node  $j$  with Rank  $L$  (or  $L$  layers) is calculated as:

$$C_{ij} = LB \times \min \left\{ \log_2 \left( 1 + \frac{P_r}{P_i + N} \right), c_{max} \right\}, \quad (2)$$

where  $B$  is the bandwidth of the link. The first term in the minimisation function is the Shannon capacity per Hz bandwidth, calculated from the bandwidth  $B$  and the signal-to-interference-plus-noise-ratio (SINR),  $P_r/(P_i + N)$ , with  $P_r$  the signal power received at the output terminal of the receiving antenna,  $P_i$  the interference power of the other signals and  $N$  the noise power, all measured in Watts (W). The second term,  $c_{max}$ , is an upper bound on the per-layer spectral efficiency. For this mmWave problem, we assume that the antennas are highly directional such that the interference power is negligible, i.e.,  $P_i \ll N$ . Thus, the SINR can be approximated by the SNR,  $P_r/N$ , and (2) can be approximated as:

$$C_{ij} \approx LB \times \min \left\{ \log_2 \left( 1 + \frac{P_r}{N} \right), c_{max} \right\}. \quad (3)$$

The received power,  $P_r$ , can be calculated using existing LoS stochastic path loss models. In this work, we consider the model in Table 7.4.1-1 of 3GPP (2022a), which can be expressed as:

$$L_p = 32.4 + 21 \log_{10}(d) + 20 \log_{10}(f_c) + L_{sf}, \quad (4)$$

where  $L_p$  is the path loss in dB,  $d$  is the distance between the Tx and the Rx in metres,  $f_c$  is the operating centre frequency in GHz, and  $L_{sf}$  is a normal random variable in dB for the shadow fading with a mean of 0 dB and a standard deviation of 4 dB.

The received power in W can be expressed as:

$$P_r = \frac{G_t G_r}{10^{(L_p/10)}} P_t, \quad (5)$$

where  $P_t$  is the power at the input terminal of the transmitting antenna in W and  $G_t$  and  $G_r$  are the gain of the transmitting antenna in the direction of the receiving antenna and the gain of the receiving antenna in the direction of the transmitting antenna, respectively.

The calculation of noise power considers only thermal noise, which can be expressed as:

$$N = k_B T B, \quad (6)$$

where  $k_B$  is the Boltzmann constant and  $T$  is the temperature in Kelvins.

Next, we give a brief introduction to the upper bound,  $c_{max}$ . The spectral efficiency of a single layer can be expressed as (3GPP, 2022b):

$$SE = \frac{RQ_m N_s}{B_{RE} t_{slot}}, \quad (7)$$

where  $R$  is the target code rate,  $Q_m$  is the modulation order,  $N_s$  is the number of symbols in each slot,  $B_{RE}$  is the bandwidth of a resource element and  $t_{slot}$  is the time duration for a slot. A 5G mmWave system supports different modulation and coding scheme tables. In this study, we consider a 64 quadrature amplitude modulation (QAM) maximum modulation scheme (3GPP, 2022b). The values of  $N_s$  and the  $B_{RE} t_{slot}$  product are fixed. Thus, the upper bound is determined by using the maximum values of  $R$  and  $Q_m$  in Table 5.1.3.1-1 of 3GPP (2022b).

Some key simulation parameters are provided in Table 1. For a given Tx-Rx pair, the received power and the link capacity are calculated based on the parameters, as well as the link length  $d$  obtained from the ray tracer implemented in Cesium.

**Table 1. Key simulation parameters in network planning.**

Parameter	Value
Operating frequency $f_c$	26 GHz
Bandwidth $B$	1 GHz
Number of layers $L$	2
Transmit power $P_t$	60 dBm
Temperature $T$	300°K
Target code rate $R$	0.926
Modulation order $Q_m$	6
Number of symbols per slot $N_s$	14
The $B_{RE} t_{slot}$ product	15
Maximum per-layer spectral efficiency $c_{max}$	5.18 bps/Hz
Maximum link length $d_{max}$	300 m
Antenna gains $G_t$ and $G_r$	0 dB
Cost of a fibre PoP	2
Cost of a relay node	1

Next, we formulate the optimisation problem as a mixed-integer linear programming problem. The objective is to select a subset of the set of fibre PoPs and potential sites (PSs) for relays in order to implement a tree-structured network that satisfies all the demands at minimum deployment cost.

We first introduce the notations used in this problem.

### Inputs to Optimisation Model

The node data is given by:

- $\mathcal{FP}$ : Set of all potential fibre PoPs.
- $\mathcal{PS}$ : Set of all potential sites to deploy relay devices.

- $\mathcal{DN}$ : Set of all demand nodes.
- $\mathcal{SS}$ : A singleton set containing a virtual super source node, which can be viewed as the gateway between the designed network and the outer network. Thus, this node is the root of the resulting tree. We assume there exists a connection between the source node and each fibre PoP with infinite capacity.
- $\mathcal{V}$ : The union of  $\mathcal{FP}$  and  $\mathcal{PS}$ .
- $K_i$ : Cost of deployment at location  $i \in \mathcal{V}$ .
- $D_i$ : Demand at demand node  $i \in \mathcal{DN}$ .

The potential link data is given by:

- $\mathcal{A}$ : Set of all possible links, including the LoS links obtained from Cesium and the virtual connections between the source and the fibre PoPs.
- $C_{ij}$ : Capacity of link  $(i, j) \in \mathcal{A}$ , where  $i, j \in \mathcal{V}$ .

### Decision Variables in Optimisation Model

The decision variables used in the optimisation problem are given by:

- $x_i$ : is 1 if node  $i \in \mathcal{V}$  is selected; 0 otherwise.
- $y_{ij}$ : is 1 if link  $(i, j) \in \mathcal{A}$  is selected; 0 otherwise.
- $f_{ij}$ : the flow from node  $i$  to node  $j$ , is positive if the flow is actually from  $i$  to  $j$ ; negative otherwise.

### Problem Formulation

The objective function is to find a subset of  $\mathcal{V}$  such that the total cost is minimised:

$$\min \sum_{i \in \mathcal{V}} K_i x_i. \tag{8}$$

The constraints are partitioned into two parts, the constraints on the flows and the constraints on the network structure.

We first discuss the former. We need to ensure that the total incoming flow equals the total outgoing flow and the demand at a node:

$$\sum_{j \in \mathcal{V} \cup \mathcal{DN} \cup \mathcal{SS}: (i,j) \in \mathcal{A}} f_{ij} + d_i = 0, \quad i \in \mathcal{V} \cup \mathcal{DN} \cup \mathcal{SS}, \tag{9}$$

where

$$d_i = \begin{cases} D_i, & i \in \mathcal{DN} \\ -M, & i \in \mathcal{SS} \\ 0, & i \in \mathcal{V} \end{cases} \tag{10}$$

with  $M = \sum_{i \in \mathcal{DN}} D_i$  denoting the total demand at all Demand Nodes (DNs).

Next, a link may only have non-zero flow when it is active:

$$|f_{ij}| \leq M y_{ij}, \quad (i, j) \in \mathcal{A}. \quad (11)$$

Furthermore, the flow in a link is upper bounded by the capacity of the link:

$$|f_{ij}| \leq C_{ij}, \quad (i, j) \in \mathcal{A}. \quad (12)$$

Constraints should also be introduced in order to ensure the tree structure of the resulting network. Since the demand nodes are leaves of the resulting tree, each demand node is covered by exactly one potential site or fibre PoP ([Jabrayilov, 2020](#)):

$$\begin{aligned} \sum_{I \in \mathcal{V}: (I, j) \in \mathcal{A}} y_{Ij} &= 1, \quad j \in \mathcal{DN}, \\ \sum_{j \in \mathcal{V}: I \in \mathcal{A}} y_{Ij} &= 1, \quad i \in \mathcal{DN}. \end{aligned} \quad (13)$$

Next, the number of links connected to a selected PS or fibre PoP must be greater than or equivalent to 2:

$$\sum_{(I, j) \in \mathcal{A}} y_{Ij} \geq 2I, \quad i \in \mathcal{V}. \quad (14)$$

Besides, the number of selected links in the resulting network is 1 less than the number of nodes. Since the number of super source nodes is 1, this constraint can be expressed as:

$$\sum_{(I, j) \in \mathcal{A}} y_{Ij} = \sum_{k \in \mathcal{V}} x_k + |\mathcal{DN}|. \quad (15)$$

Finally, a node variable is set to one as long as a link it connects to is taken into the solution:

$$\begin{aligned} y_{ij} &\leq x_I, \quad i \in \mathcal{V}, I \in \mathcal{A}, \\ y_{ij} &\leq x_j, \quad j \in \mathcal{V}, I(i, j) \in \mathcal{A}. \end{aligned} \quad (16)$$

As we can see in the constraints, decision variables  $y_{ij}$  for the links and  $f_{ij}$  for the flows are introduced. In order to formulate this problem as a linear programming problem, we restate the objective function in (8) as:

$$\text{Min } \sum_{i \in \mathcal{V}} K_i x_i + \sum_{(I, j) \in \mathcal{A}} \delta y_{Ij} + \sum_{I \in \mathcal{A}} \epsilon f_{Ij}, \quad (17)$$

where  $\delta$  and  $\epsilon$  are small values denoting the “costs” of a link and a flow, respectively. Notice that  $\epsilon \ll \delta$  since the  $f_{ij}$  are usually of the order of  $10^6$  up to  $10^{10}$ , while  $y_{ij}$  is binary. Although (17) increases the dimension of the problem by  $2|\mathcal{A}|$ , the problem can now be solved using a mixed-integer linear programming solver. The solver we consider is Matlab function “*intlinprog()*” ([MathWorks, 2019](#)) from the Optimisation Toolbox. It takes the potential node locations and links, as well as the metrics calculated in Cesium as inputs, and exports the optimisation results back to Cesium for visualisation.

## Case Study and Result Analysis

### LoS Probability Validation

#### Case Study

Two sets of simulations are performed to verify the urban area LoS probability model in (1) and study the possible factors that affect the parameters. Firstly, simulations are performed in different 3D city models, namely Melbourne, Adelaide and Darwin, in order to investigate the relationship between the parameters and the density of the buildings. For this set of simulations, we only consider the ground-to-ground LoS probability. In other words, the Tx's and Rx's must be placed at ground level. The regions where the simulations are performed are shown by the red regions in Figures 4, 5 and 6.

Apart from cities, the height can also affect the building density. In order to investigate how the Tx height impacts the parameters in (1), another set of simulations are performed in the 3D model of Melbourne, shown in Figure 4. The Tx is placed at a certain longitude and latitude with different heights above ground level, while the Rx locations are randomly selected at ground level. The Tx location is given by the green spot in Figure 4.



Figure 4. Region for simulation in Melbourne.



Figure 5. Region for simulation in Adelaide.



Figure 6. Region for simulation in Darwin.

## Results and Analysis

Figure 7 shows the LoS probability versus distance in Melbourne, Adelaide and Darwin. The curves in dashed lines are the simulation results, while those in solid lines are fitted curves based on the simulations results and (1). The corresponding parameters of the fitted curves are given in Table 2. We observe that the threshold distances for Darwin and Melbourne are 0, while the value for Adelaide is 2. Since the Tx is always located at ground level, the value of  $A$  is expected to be 0. Nevertheless, since this does not make significant difference between the fitted curves for Melbourne and Adelaide, we consider this difference in  $A$  as an insignificant error in fitting results. In addition, the parameter  $E$  for Darwin is much larger than for the other two cities, which makes the curve decay more slowly. As can be observed in



Figures 4, 5 and 6, the density of the buildings in Darwin is lower than in Melbourne and Adelaide. Therefore, we conclude that the parameter  $E$  related to the decaying speed decreases with increasing building density.

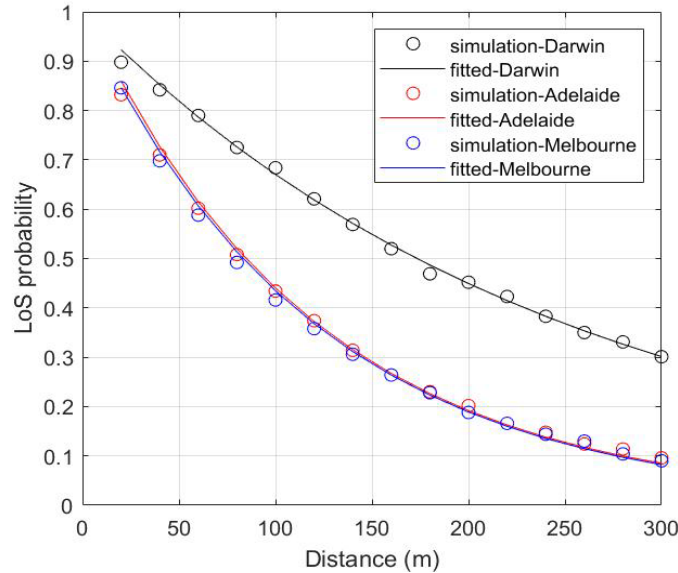


Figure 7. LoS probability versus distance in Melbourne, Adelaide and Darwin.

Table 2. Fitted parameters for different cities.

City	$A$ (metres)	$E$ (metres)
Melbourne	0	120
Adelaide	2	118
Darwin	0	250

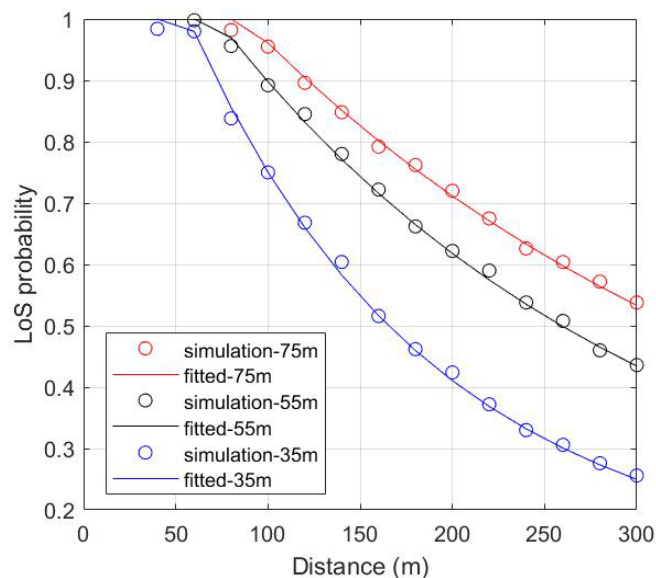


Figure 8. LoS probability versus distance in Melbourne. The Tx is placed at a certain location, 35 m, 55 m or 75 m above ground level.

Figure 8 shows the LoS probability versus distance for different Tx heights. The corresponding parameters are given in Table 3. Both  $A$  and  $E$  increase with increasing Tx height. The

threshold  $A$  increases since the Rx's are placed at ground level; thus, no LoS probability results below a certain distance are available. The parameter  $E$  increases since the density of the buildings usually decreases with the height.

**Table 3. Fitted parameters for different Tx heights.**

Tx height (metres)	$A$ (metres)	$E$ (metres)
35	57	115
55	72	220
75	87	280

## Deployment Cost Optimisation in Network Planning

### Case Study

As introduced in the section on development of [deployment cost optimisation](#), communication is possible between certain types of site pairs. An example of the node locations and potential links is given in Figure 9, in which a part of downtown Melbourne is considered as the region of interest.

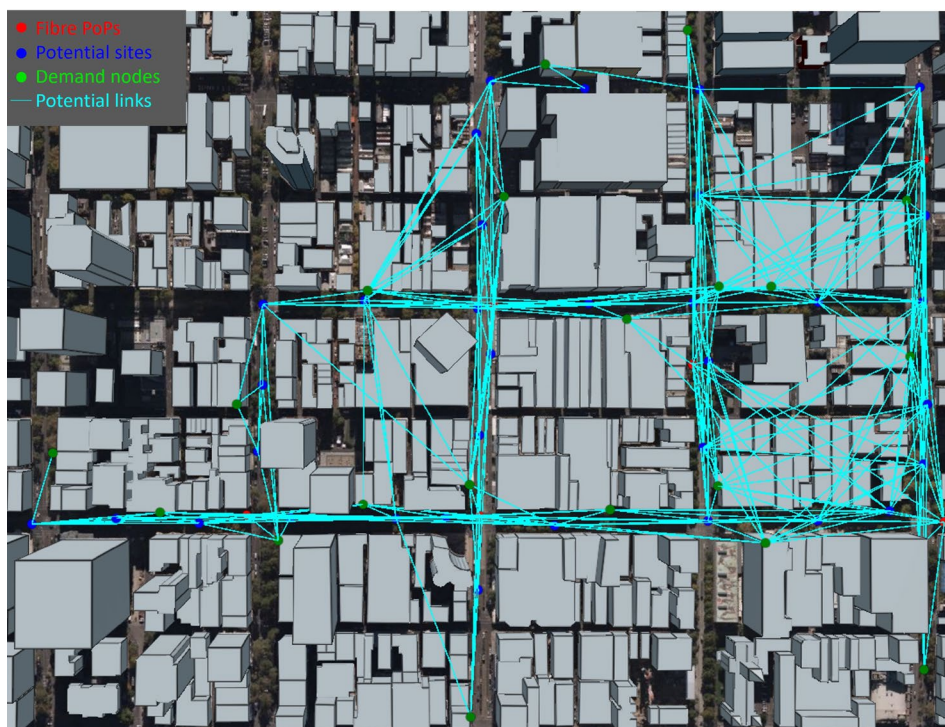


**Figure 9. Potential LoS links (cyan lines) obtained from the given fibre PoPs (red dots), PSs (blue dots) and DNs (green dots).**

As is discussed in the section on prototype [data](#), the potential site locations are manually selected, since these datasets are not available. In order to approximate a practical scenario, we define the following rules for the selection of potential sites:

- A fibre PoP or a PS must be located on a streetlight. In other words, these nodes must be placed on the street with a certain height above the ground.

- A DN must be located at the edge of the rooftop of a building. As such, the total demand of all users in a given building is represented by the demand of this node.

## Results and Analysis

Using the node locations and potential links given in Figure 9 as the optimisation input, the resulting network is shown by the lawn-green lines in Figure 10. The network is divided into two parts: each of them is a tree with a fibre PoP as the root. By connecting the two selected fibre PoPs to the virtual source node, the resulting network is tree structured.

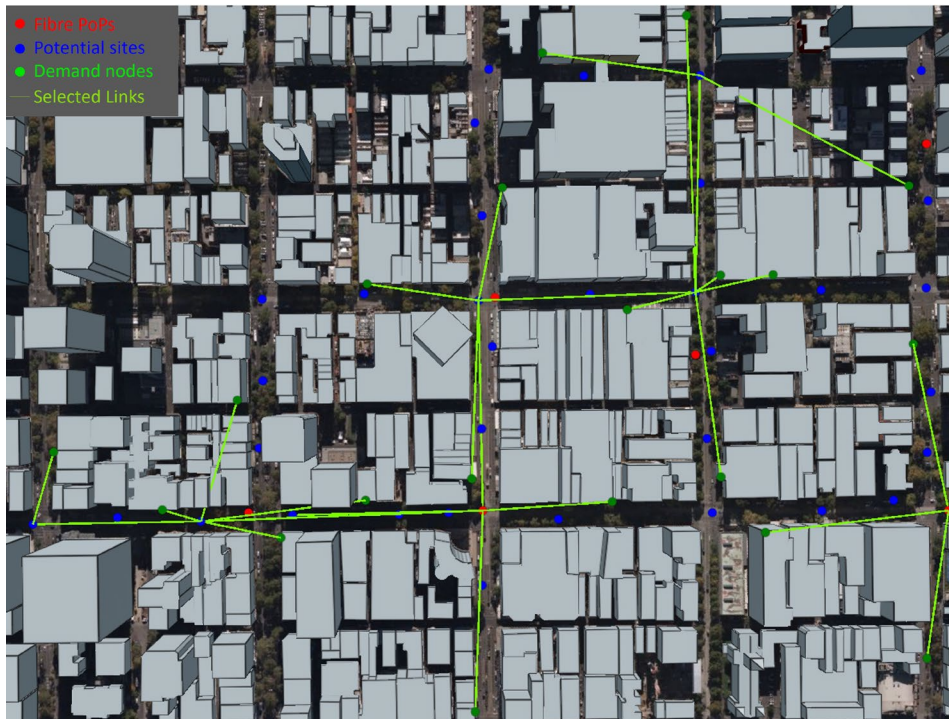


**Figure 10** The selected links (lawn green lines) resulting from the optimisation problem. The input of the optimisation problem is visualised in Figure 9.

Apart from the solution to the optimisation problem, the time required to solve it is also of great interest, as we would like to know if we should partition the problem into subproblems when the size is large. Figure 11 plots the simulation time required to solve the problem with the dimension of the problem using black circles. The time required for optimisation increases slowly in the low dimension region and rises quickly in the high dimension region.

The mixed-integer linear programming problem is known to be an NP hard problem. Though it is still not known if an NP hard problem can be solved in polynomial time, we try to fit the points using a polynomial curve. It is shown in Figure 11 by a blue dashed line that a polynomial fit with degree of 7 is very close to the simulation time. The fitted curve can be expressed as:

$$f(x) = 1.32 \times 10^{-16}x^7 - 3.228 \times 10^{-13}x^6 + 3.126 \times 10^{-10}x^5 - 1.506 \times 10^{-7}x^4 + 3.827 \times 10^{-5}x^3 - 5.001 \times 10^{-3}x^2 + 0.302x - 5.628. \quad (18)$$

This result might be useful when we would like to predict the optimisation time for higher dimensional problems.

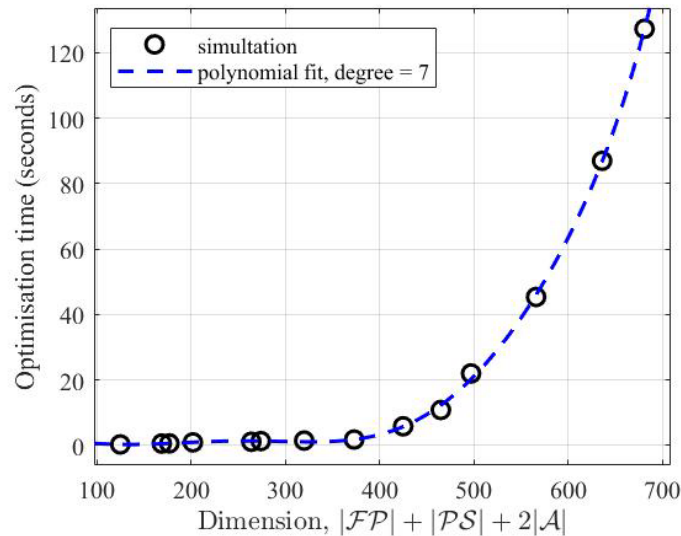


Figure 11. Time for solving the optimisation problem (black circles) and the polynomial fit (blue dashed line) in (18).

## Conclusions and Future Extensions

The contribution of this paper includes the validation of an existing LoS probability model and the development of an urban area site location selection tool based on 3D city models. More specifically, we developed a simple ray tracer in Cesium in which only LoS paths are considered. Based on its LoS checking functionality, we validated an LoS probability model expressed as an exponential rule with the link length. By fitting the simulation results in different scenarios to the model, we found that the decaying speed of this exponential function increases with the building density, while the threshold distance increases with the Tx height. In addition, we develop a network planning tool by formulating a mixed-integer linear programming problem in order to minimise the overall deployment cost by optimal site selection. The ray tracer first checks potential LoS links and provides the length of each link to enable the calculation of the link capacity. The potential locations of the nodes are manually generated due to the limitation of the 3D dataset. Taking the sets of site locations and potential links as the inputs, an existing Matlab solver is used to select a subset of the sites in order to construct a tree-structured network that satisfies all the user demands at a minimum deployment cost. The optimisation results are then sent back to Cesium for visualisation. We also analyse the time required for solving this optimisation problem in order to provide a prediction to the optimisation time for larger sized problems.

In the following points, we outline several possible directions for further work.

- The 3D geospatial dataset we are using does not contain street furniture and vegetation. It would be desirable if 3D data with these features are available. With street furniture, it would be possible to automate the process of inspecting the fibre PoP and PS locations based on 3D computer vision and machine learning techniques (Danford *et al.*, 2017). As such, it will be easier to investigate the capability of the network planning tool with increasing problem dimension. With vegetation in the data, the foliage loss can be taken into consideration when calculating the path loss (ITU, 2016). Besides, we can use the ray tracer to evaluate other LoS probability models such as NYU-squared model in which foliage is considered (Aalto *et al.*, 2016).
- Though LoS transmission plays a major role in mmWave communications, the ray tracer could be extended to include specular reflections. By considering multi-path components, highly accurate characterisation of the received signal can be achieved, including phase shift, power and Angle of Arrival. The specular reflected paths are usually calculated using the method of images, which is computationally costly (Lecci *et al.*, 2021). Therefore, it is important to understand the tradeoffs between the accuracy and the efficiency in RT.
- In the modified objective function in (17), the problem dimension is increased to  $|\mathcal{FP}| + |\mathcal{PS}| + 2|\mathcal{A}|$  compared to the original problem in (8), in order to formulate the problem as a mixed-integer linear programming problem. Since the mixed-integer linear programming problem is known to be NP hard, it would be desirable to come up with a problem formulation in which the dimension is the same as the original problem.

## References

- 3rd Generation Partnership Project (3GPP). (2022a). Physical layer procedures for data. No. 38.214 Version 17.2.0. Technical specification. Available from <https://portal.3gpp.org/desktopmodules/Specifications/SpecificationDetails.aspx?specificationId=3216>.
- 3rd Generation Partnership Project (3GPP). (2022b). Study on channel model for frequencies from 0.5 to 100 GHz. No. 38.901 Version 17.0.0. Technical report. Available from <https://portal.3gpp.org/desktopmodules/Specifications/SpecificationDetails.aspx?specificationId=3173>.
- Aalto University, AT&T, BUPT, CMCC, Ericsson, Huawei, Intel, KT Corporation, Nokia, NTT DOCOMO, New York University, Qualcomm, Samsung, University of Bristol, & University of Southern California. (2016). 5G channel model for bands up to 100 GHz. Version 2.3. Available from <http://www.5gworkshops.com/5GCM.html>.
- Al-Hourani, A. (2020). On the probability of line-of-sight in urban environments. *IEEE Wireless Communications Letters*, 9(8), 1178–1181. <http://doi.org/10.1109/LWC.2020.2984497>.

- Andrews, J. G., Bai, T., Kulkarni, M. N., Alkhateeb, A., Gupta, A K., & Heath, R W. (2017). Modeling and analyzing millimeter wave cellular systems. *IEEE Transactions on Communications*, 64(1), 403–430. <http://doi.org/10.1109/TCOMM.2016.2618794>.
- Anjinappa, C. K., Erden, F., & Guvenc, I. (2021). Base station and passive reflectors placement for urban mmWave networks. *IEEE Transactions on Vehicular Technology*, 70(4), 3525–3539. <http://doi.org/10.1109/TVT.2021.3065221>.
- Ashour, M., Ibrahim, M., Elhoshy, S., Megalli, Y., El-Shabrawy, T., Hammad, H., & Rizk, M. R. M. (2016). A fast ray tracing algorithm for network planning based on relative coverage computations. In 2016 International Conference on Selected Topics in Mobile Wireless Networking (MoWNeT). <http://doi.org/10.1109/MoWNet.2016.7496621>.
- Bai, T., Vaze, R., & Heath, R W. (2014). Analysis of blockage effects on urban cellular Networks. *IEEE Transactions on Wireless Communications*, 13(9), 5070–5083. <http://doi.org/10.1109/TWC.2014.2331971>.
- Baum, D., Hansen, J., Salo, J., Del Galdo, G., Milojevic, M., & Kyosti, P. (2005). An interim channel model for beyond-3G systems: extending the 3GPP spatial channel model (SCM). In 2005 IEEE 61st Vehicular Technology Conference, 5, 3132–3136. <http://doi.org/10.1109/VETECS.2005.1543924>.
- Benyamina, D., Hafid, A., & Gendreau, M. (2012). Wireless mesh networks design — A survey. *IEEE Communications Surveys & Tutorials*, 14(2), 299–310. <http://doi.org/10.1109/SURV.2011.042711.00007>.
- Bodi, A., Blandino, S., Varshney, N., Zhang, J., Ropitault, T., Lecci, M., Testolina, P., Wang, J., Lai, C., & Gentile, C. (2021). NIST Quasi-deterministic channel realization software documentation. [Internet]. Available from <https://github.com/wigig-tools/qd-realization/blob/master/docs/Documentation.pdf>
- Cesium. (2015a). The Cesium Platform. [Internet]. Available from <https://cesium.com/platform/>
- Cesium. (2015b). Cesium OSM Buildings. [Internet]. Available from <https://cesium.com/platform/cesium-ion/content/cesium-osm-buildings/>.
- Choubey, N., & Yazdan, A. (2016). Introducing Facebook’s new terrestrial connectivity systems — Terragraph and Project ARIES. [Internet]. Available from <https://engineering.fb.com/2016/04/13/connectivity/introducing-facebook-s-new-terrestrial-connectivity-systems-terragraph-and-project-aries/>.
- Cui, Z., Guan, K., Briso-Rodriguez, C., Ai, B., & Zhong, Z. (2020). Frequency-dependent line-of-sight probability modeling in built-up environments. *IEEE Internet of Things Journal*, 7(1), 699–709. <http://doi.org/10.1109/JIOT.2019.2947782>.
- Danford, T., Filiz, O., Huang, J., Karrer, B., Paluri, M., Pang, G., Ponnampalam, V., Stier-Moses, N., & Tezel, B. (2017). End-to-end planning of fixed millimeter-wave networks. arXiv. Available from <https://arxiv.org/abs/1705.07249>.
- He, D., Ai, B., Guan, K., Wang, L., Zhong, Z., & Kurner, T. (2019). The design and applications of high-performance ray-tracing simulation platform for 5G and beyond wireless communications: A tutorial. *IEEE Communications Surveys & Tutorials*, 21(1), 10–27. <http://doi.org/10.1109/COMST.2018.2865724>.

- International Telecommunication Union (ITU). (2021). Attenuation in vegetation. Number P.833-10. Available from <https://www.itu.int/rec/R-REC-P.833/en>.
- Jabrayilov, A. (2020). On the hop-constrained Steiner tree problems. arXiv. Available from <https://arxiv.org/abs/2007.07405>
- Jamsa, T., Medbo, J., Kyosti, P., Haneda, K., & Raschkowski, L. (2016). The 5G wireless propagation channel models. In M. Dohler & T. Nakamura (Authors) & A. Osseiran, J. Monserrat & P. Marsch (Eds.), *5G Mobile and Wireless Communications Technology* (pp. 357–380). Cambridge: Cambridge University Press. <https://doi.org/10.1017/CBO9781316417744.014>
- Kennington, J. L., Olinick, E., & Rajan, D. (2011). *Wireless Network Design: Optimization Models and Solution Procedures*. Springer.
- Lai, C., Sun, R., Gentile, C., Papazian, P. B., Wang, J., & Senic, J. (2019). Methodology for multipath-component tracking in millimeter-Wave Channel modeling. *IEEE Transactions on Antennas and Propagation*, 67(3), 1826–1836. <http://doi.org/10.1109/TAP.2018.2888686>.
- Lalwani, S. (2018). Economics of Terragraph Backhaul for ATT's 5G network in San Jose. [Internet]. Available from <https://www.digitaltwinsim.com/terragraph>.
- Lecci, M., Testolina, P., Giordani, M., Polese, M., Ropitault, T., Gentile, C., Varshney, N., Bodi, A., & Zorzi, M. (2020). Simplified ray tracing for the millimeter wave channel: A performance evaluation. 2020 Information Theory and Applications Workshop (ITA). <http://doi.org/10.1109/ITA50056.2020.9244950>.
- Lecci, M., Testolina, P., Polese, M., Giordani, M., & Zorzi, M. (2021). Accuracy versus complexity for mmWave ray-tracing: A full stack perspective. *IEEE Transactions on Wireless Communications*, 20(12), 7826–7841. <http://doi.org/10.1109/TWC.2021.3088349>.
- MathWorks. (2019). intlinprog Mixed-integer linear programming (MILP). [Internet]. Available from <https://au.mathworks.com/help/optim/ug/intlinprog.html>.
- MathWorks. (2022). Optimization Toolbox. [Internet]. Available from [https://au.mathworks.com/help/optim/index.html?s\\_tid=CRUX\\_lftnav](https://au.mathworks.com/help/optim/index.html?s_tid=CRUX_lftnav).
- McKown, J., & Hamilton, R. (1991). Ray tracing as a design tool for radio networks. *IEEE Network*, 5(6), 27–30. <http://doi.org/10.1109/65.103807>.
- Meinila, J., Kyosti, P., Jamsa, T., & Hentila, L. (2009). WINNER II Channel Models. In M. Döttling, W. Mohr & A. Osseiran (Eds.), *Radio Technologies and Concepts for IMT-Advanced* (pp. 357–380). John Wiley & Sons. <https://doi.org/10.1002/9780470748077.ch3>
- Mellios, E., Nix, A. R., & Hilton, G. S. (2012). Ray-tracing urban macrocell propagation statistics and comparison with WINNER II/+ measurements and models. In 2012 Loughborough Antennas Propagation Conference (LAPC). <http://doi.org/10.1109/LAPC.2012.6403073>.
- Rangan, S., Rappaport, T. S., & Erkip, E. (2014). Millimeter-wave cellular wireless networks: Potentials and challenges. *Proceedings of the IEEE*, 102(3), 366–385. <http://doi.org/10.1109/JPROC.2014.2299397>.

- Rappaport, T. S., Sun, S., Mayzus, R., Zhao, H., Azar, Y., Wang, K., Wong, G. N., Schulz, J. K., Samimi, M., & Gutierrez, F. (2013). Millimeter wave mobile communications for 5G cellular: It will work!. *IEEE Access*, 1, 335–349. <http://doi.org/10.1109/ACCESS.2013.2260813>.
- Thomas, T. A., Rybakowski, M., & Krysiak, P. (2016). Preliminary 5G suburban micro (SMi) channel model for different foliage conditions. In 2016 IEEE Globecom Workshops (GC Wkshps). <http://doi.org/10.1109/GLOCOMW.2016.7849007>.
- Thomas, T. A., & Vook, F. W. (2014). System level modeling and performance of an outdoor mmWave local area access system. In 2014 IEEE 25th Annual International Symposium on Personal, Indoor, and Mobile Radio Communication (PIMRC). <http://doi.org/10.1109/PIMRC.2014.7136142>.
- Winter, P. (1987). Steiner problem in networks: A survey. *Networks*, 17(2), 129–167. <https://doi.org/10.1002/net.3230170203>.
- Zhang, Z., Ryu, J., Subramanian, S., & Sampath, A. (2015). Coverage and channel characteristics of millimeter wave band using ray tracing. In 2015 IEEE International Conference on Communications (ICC). <http://doi.org/10.1109/ICC.2015.7248516>.